Hindawi
International Journal of Antennas and Propagation
Volume 2022, Article ID 1496851, 10 pages
https://doi.org/10.1155/2022/1496851

Research Article

A Wideband Feed Network for Vivaldi Antenna Arrays

Natasha Antoinette Hall, Johann Wilhelm Odendaal, and Johan Joubert

Centre for Electromagnetism, Department of Electrical, Electronic and Computer Engineering, University of Pretoria, Pretoria 0002, South Africa

Correspondence should be addressed to Johann Wilhelm Odendaal; wimpie@up.ac.za

Received 13 July 2022; Accepted 24 August 2022; Published 10 September 2022

Academic Editor: Muhammad Zubair

A wideband feed network for a Vivaldi antenna array is presented. A limitation of current wideband antenna arrays is the bandwidth of either the feed network or the antenna element. The proposed antenna array consists of four wideband Vivaldi antennas fed with an improved wideband feed network to extend the useable bandwidth of the array. The proposed feed network consists of coplanar waveguide-to-slotline-to-microstrip line transitions. The feed network has a single coplanar waveguide input and four microstrip line output ports. The feed network achieved uniform amplitude and phase balance and an impedance bandwidth of 160% from 1 GHz to 9 GHz. The feed network was used in a uniform linear antenna array to feed four Vivaldi antenna elements. The Vivaldi antenna array achieved stable radiation patterns from 1.3 GHz to 8 GHz, resulting in a useable bandwidth of 144%. The antenna array has a minimum gain of 8 dBi and a maximum of 13.8 dBi within the frequency band. Results for a prototype Vivaldi antenna array, measured in a compact antenna test range, are presented and compared to simulated results from CST Studio Suite.

1. Introduction

Vivaldi antennas are typically used in wideband applications, viz., ground penetrating radars, wideband radar imaging, radio astronomy [1], and multiband communication systems (5G). The inherent bandwidth limitation of corporate feed networks limits the use of Vivaldi antenna elements in wideband arrays. Current feed networks for arrays include a self-matching feed network with a simple structure, but generally exhibit a narrow bandwidth. Using this feed network to feed rectangular patch elements, a relative impedance bandwidth of 10.7% was achieved [2]. A number of papers presented combinations of microstrip-to-slotline transitions to realize wideband feed networks [3–5]. These feed networks were combined with different radiation elements to realize wideband arrays, e.g., patch elements to achieve a bandwidth of 5.7% [3], UWB monopoles with a bandwidth of approximately 89% [4], and also Vivaldi antenna elements with a bandwidth of 84% [5]. Other similar wideband antenna arrays include the use of multiple substrate layered feed networks such as substrate-integrated waveguide (SIW) [6, 7] and an electromagnetic band gap (EBG) power divider [8] used to feed different patch elements. These antenna arrays achieved bandwidths between 20% and 50%.

Individual Vivaldi antennas are generally capable of achieving bandwidths in excess of 100% [9], while current implementations of wideband arrays only demonstrate bandwidths of 80% to 90%. This paper presents a wideband corporate feed network with more than 160% impedance bandwidth from 1 GHz to 9 GHz. The wideband properties of microstrip-to-slotline transitions are exploited to design a four element corporate feed network. The proposed coplanar waveguide (CPW) fed network consists of a CPW-to-slotline transition and two slotline-to-microstrip line transitions to realize a uniform linear antenna array of four Vivaldi antenna elements. The Vivaldi antenna array achieved stable radiation patterns from 1.3 GHz to 8 GHz, resulting in a useable bandwidth of 144%.

The design and performance of the feed network and a single Vivaldi antenna element are presented in Section 2. Section 3 presents the measured and simulated results for the final antenna array, with concluding remarks in Section 4.

2. Feed Network and Vivaldi Element

2.1. Wideband Feed Network. The top and bottom sides of the proposed feed network are shown in Figure 1 and consist of a CPW-to-slotline transition and two slotline-to-microstrip line transitions. The feed network was implemented on Rogers RO4003C substrate with a height of $h = 1.524$ mm and was simulated in CST Studio Suite [10]. Port 1 of the feed network consists of a CPW line with a characteristic impedance of $Z_{0\mathrm{CPW}} = 50\,\Omega$ that transitions into two slotlines, each with a characteristic impedance of $Z_{0\mathrm{SL}} = 119\,\Omega$. Slotline-to-microstrip line transitions are employed to realize four microstrip ports with characteristic impedances of $Z_{0\mathrm{MSL}} = 50\,\Omega$.

In order to realize a uniform, equally spaced Vivaldi antenna array structure, and to mitigate grating lobes in the radiation pattern, the distance between the antenna elements were chosen as $d = 0.65\lambda_0$ with λ_0 the free space wavelength at a frequency of 5.5 GHz. The 180° phase difference between ports 2 and 3, and ports 4 and 5, was mitigated by changing the polarity/orientation of the two inner Vivaldi elements. To ensure that the distance between the conductor sides of the Vivaldi radiating elements are equal, small offsets were introduced in the distances between the microstrip ports resulting in d_1, d_2, and d_3 in Figure 1. The different slotline-to-microstrip transitions were optimized for maximum input impedance bandwidth. To realize uniform and in-phase array excitations, the physical lengths of the microstrip line section must be equal. This was obtained by implementing different radiuses for the two different microstrip line sections. The dimensions for the final feed network are given in Table 1 and a prototype of the feed network is shown in Figure 2.

The *S*-parameters of the prototype feed network were measured with a HP8510C vector network analyzer. The simulated and measured reflection coefficients for port 1 are shown in Figure 3, with an impedance bandwidth from 1 GHz to 9 GHz. The simulated and measured reflection coefficients agree reasonably well with the differences probably due to manufacturing accuracy, especially the width and radial curves of the CPW and slotlines. The magnitudes and phases of the transmission coefficients for the feed network are presented in Figures 4 and 5, respectively. The magnitudes of the different transmission parameters are approximately the same with some losses visible for the frequencies above 6 GHz. This is probably due to the large radial stubs required to increase the bandwidth. The measured and simulated phases at ports 2 and 3 are almost the same with a 180° difference between the 2 ports. The transmission parameters for ports 4 and 5 are similar to that of ports 2 and 3.

2.2. Vivaldi Antenna Element. The exponentially tapered Vivaldi antenna element was implemented on RO4003 C substrate with a height of $h = 1.524$ mm and is shown in Figure 6 with final dimensions in Table 2. The simulated and measured reflection coefficients for a Vivaldi antenna element are given in Figure 7. The impedance bandwidth, for a −10 dB reflection coefficient, of the single Vivaldi antenna was from 1.1 GHz to 9.5 GHz. Four Vivaldi elements were manufactured and all obtained similar results.

3. Linear Vivaldi Antenna Array

The assembled uniform linear Vivaldi array mounted on the pedestal of a compact antenna test range is shown in Figure 8. The measured and simulated *S*-parameter results for the complete antenna array are shown in Figure 9. The impedance bandwidth is from 1.3 GHz to 9 GHz with a reflection coefficient response below −10 dB with some minor exceptions. The VSWR for the entire frequency range was below 2.5 : 1. The simulated and measured reflection coefficients agree reasonably well except for some frequencies close to 4 GHz. The simulated values for the reflection coefficient are significantly lower than the measured values. Possible reasons for these differences can be attributed to small manufacturing or assembling differences between the prototype array and the ideal simulation model and/or interaction between the array and the measurement environment. The realized gain of the array on boresight was above 8 dBi between 1.5 GHz and 8 GHz, with a maximum of 13.8 dBi at 6.3 GHz, as shown in Figure 10. Above 8 GHz, the boresight gain decreases significantly due to a deterioration of the main beam of the individual Vivaldi antennas. The simulated total efficiency of the antenna array is shown in Figure 11. The total efficiency of the array is above 83% within the useable frequency range of 1.3 GHz to 8 GHz.

The *E*- and *H*-plane radiation patterns at discrete frequencies are presented in Figures 12–14. The measured and simulated results were similar with the cross-polarization for all frequencies below −10 dB in the main beam. Stable radiation patterns with well-defined main beams were obtained for frequencies up to 8 GHz. Although the feed network achieved an impedance bandwidth of 160%, the useable bandwidth of the array with stable radiation patterns is limited to a 144% bandwidth from 1.3 GHz to 8 GHz.

Table 3 compares the performance of the proposed wideband Vivaldi antenna array with similar wideband arrays in the literature [4–8]. The proposed array in this paper achieved a wider useable bandwidth as well as a higher maximum gain compared to [4, 5], which has a similar single layer feed network structure. The array structures in [6–8] utilize multilayer feed networks such as a substrate-integrated waveguide (SIW) or an electromagnetic band gap (EBG) structure power divider. The advantage of these array structures is that they are more compact than the proposed array, however, the bandwidths achieved are less than that of the proposed antenna array.

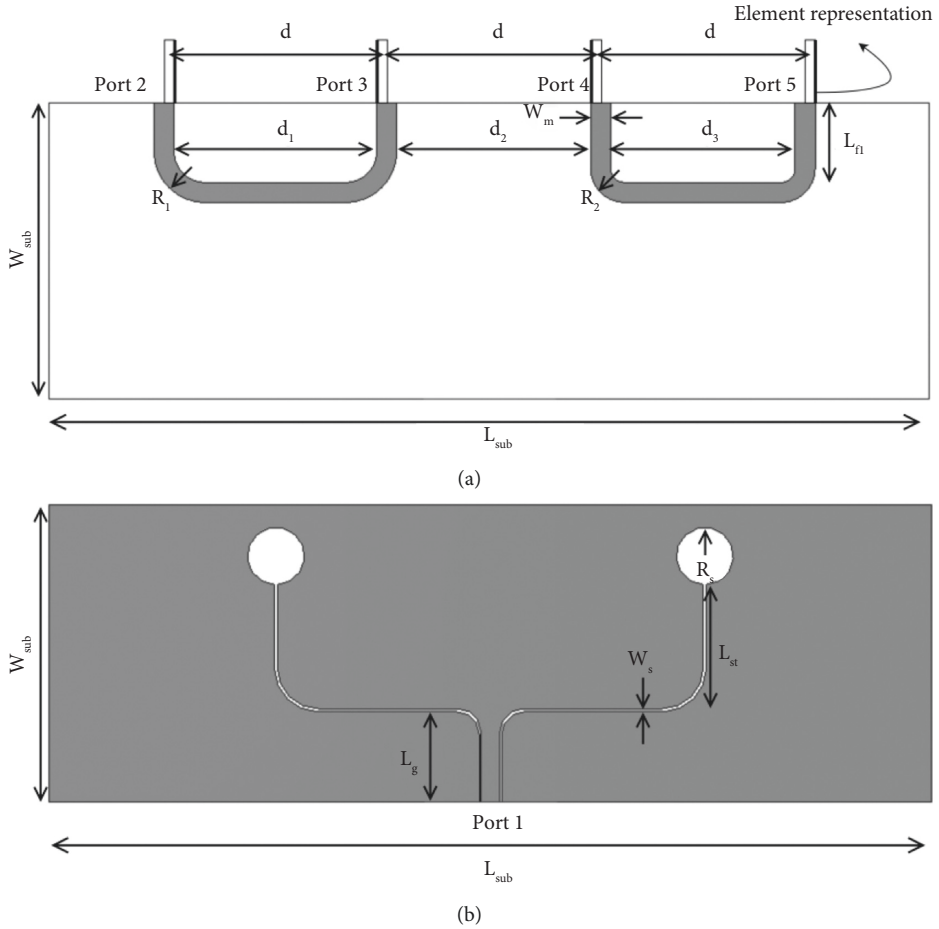

Figure 1: The top and bottom sides of the proposed feed network. (a) Top view. (b) Bottom view.

Table 1: Parameters for the final feed network.

Symbol	Description	Value (mm)
d_1	Distance between ports 2 and 3	35.61
d_2	Distance between ports 3 and 4	34
d_3	Distance between ports 4 and 5	32.39
L_{f1}	Length of vertical microstrip line	14
L_g	Length of CPW line	16
L_{st}	Length of vertical slotline	21.7
L_{sub}	Substrate length	51.95
R_1	Radius of one microstrip line turn section	8.75
R_2	Radius of the other microstrip line turn section	6
R_s	Radius of circular slot stub	5
W_m	Width of microstrip line	3.53
W_s	Width of slotline	0.5
W_{sub}	Substrate width	154.56

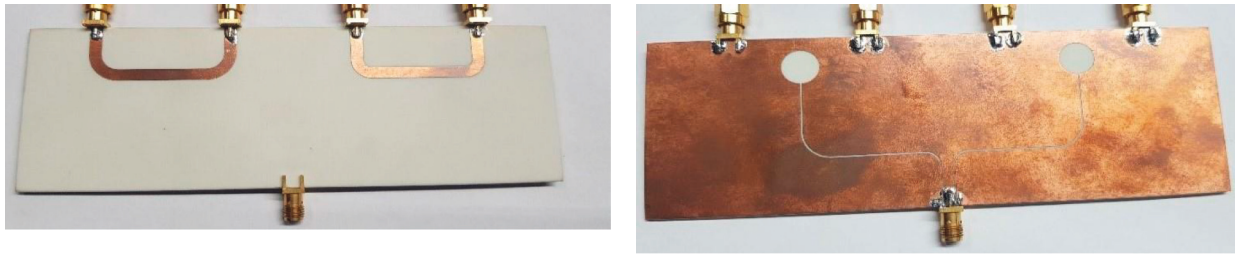

(a) (b)

Figure 2: The top and bottom sides of the prototype feed network. (a) Top plane. (b) Bottom plane.

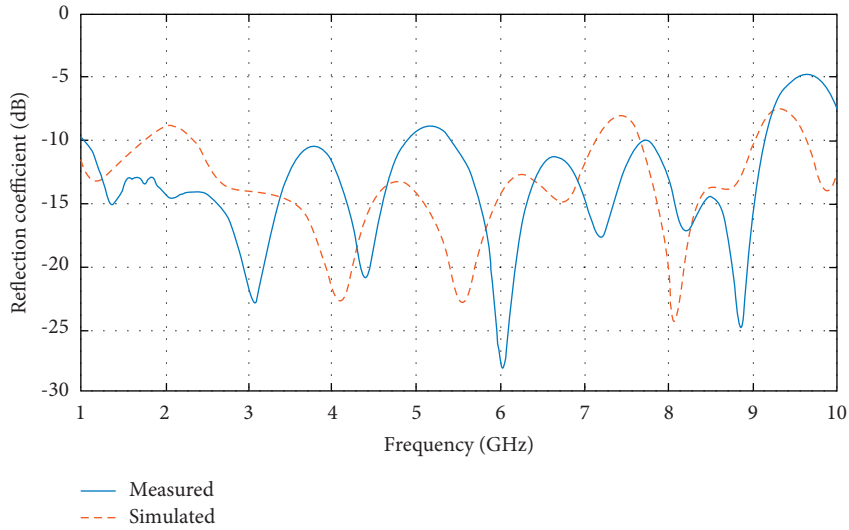

Figure 3: Measured and simulated reflection coefficients for port 1 of the feed network.

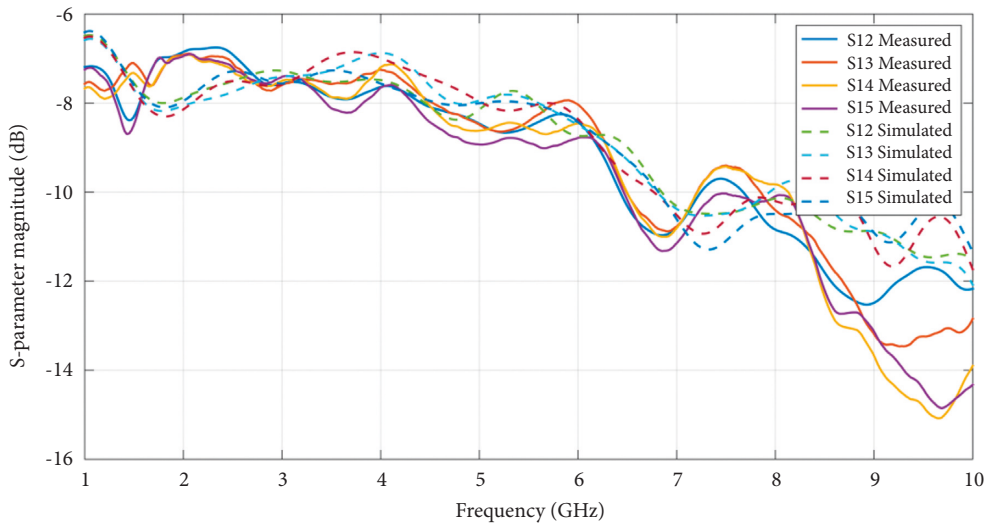

Figure 4: Measured and simulated magnitudes of the transmission coefficients for the feed network.

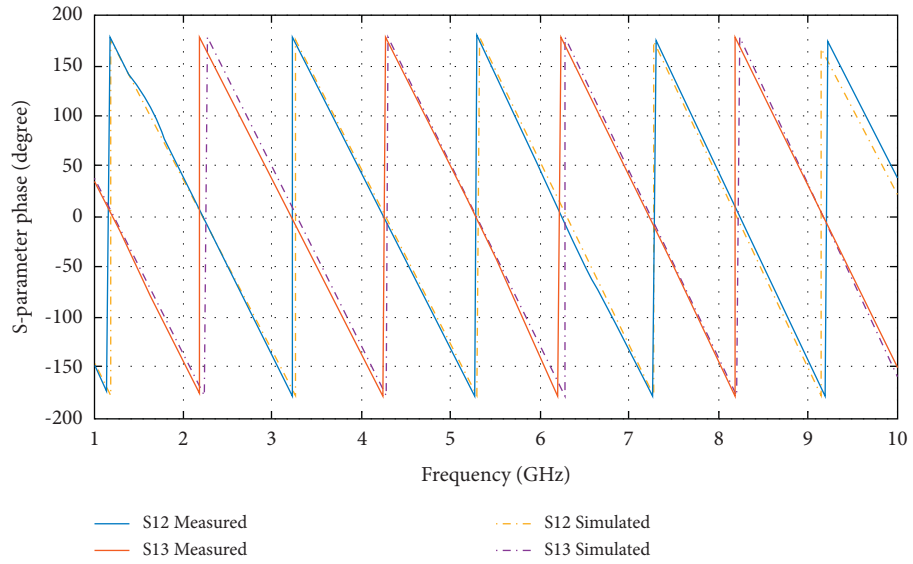

Figure 5: Measured and simulated phases of the transmission coefficients for the feed network.

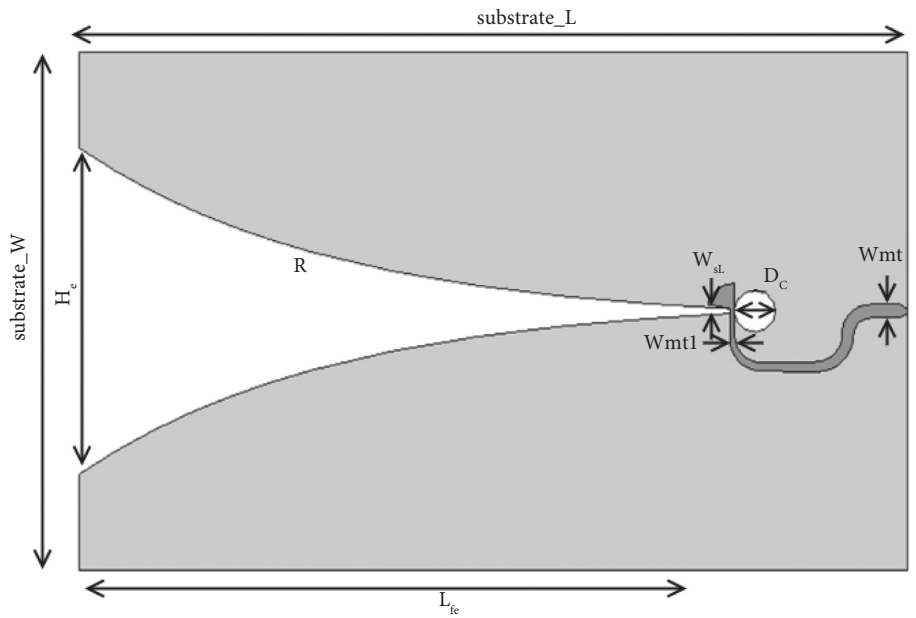

Figure 6: Vivaldi antenna element.

Table 2: Dimensions for the wideband Vivaldi antenna element.

Symbol	Description	Value (mm)
D_c	Diameter of circular slot stub	10.78
H_e	Width of Vivaldi aperture	82
L_{fe}	Length of Vivaldi taper	158.76
R	Vivaldi taper rate	$15e-3$
substrate_L	Substrate length	209.76
substrate_W	Substrate width	135
Wmt	Width of the microstrip line at the port	3.53
Wmt1	Width of the microstrip line at the transition	1.22
W_{sL}	Width of slotline	0.6

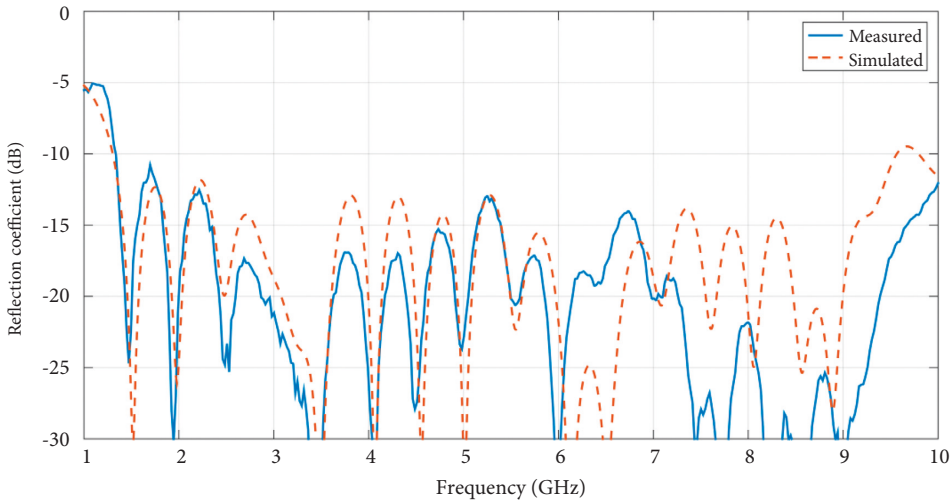

Figure 7: The simulated and measured reflection coefficient for the Vivaldi antenna element.

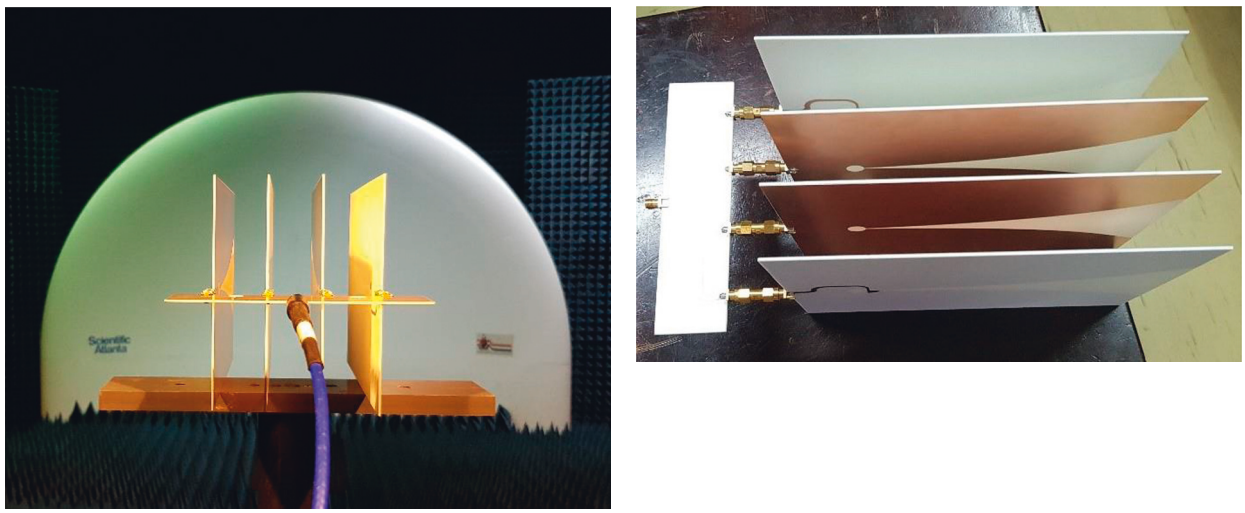

(a) (b)

Figure 8: Images of the proposed prototype antenna array. (a) Prototype antenna array in compact antenna range. (b) Prototype antenna array.

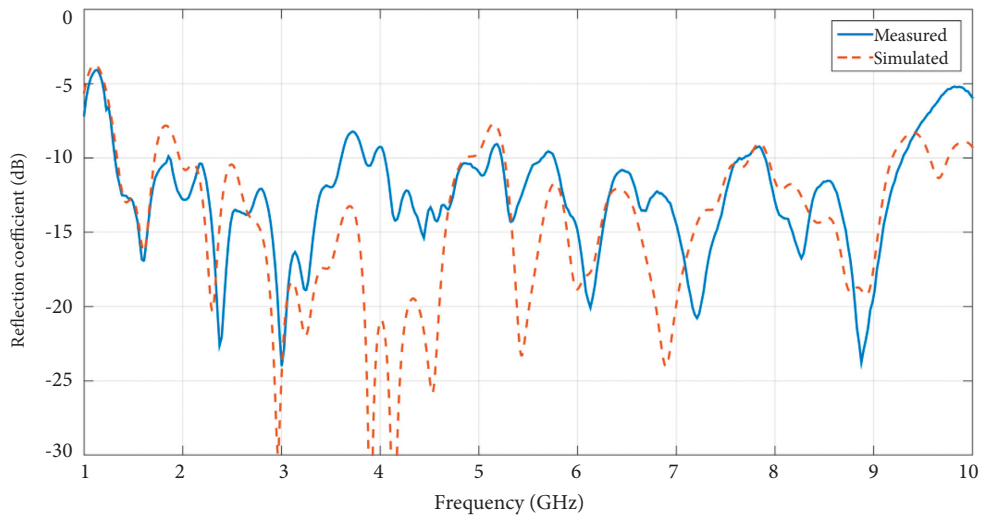

Figure 9: The simulated and measured reflection coefficient for the antenna array.

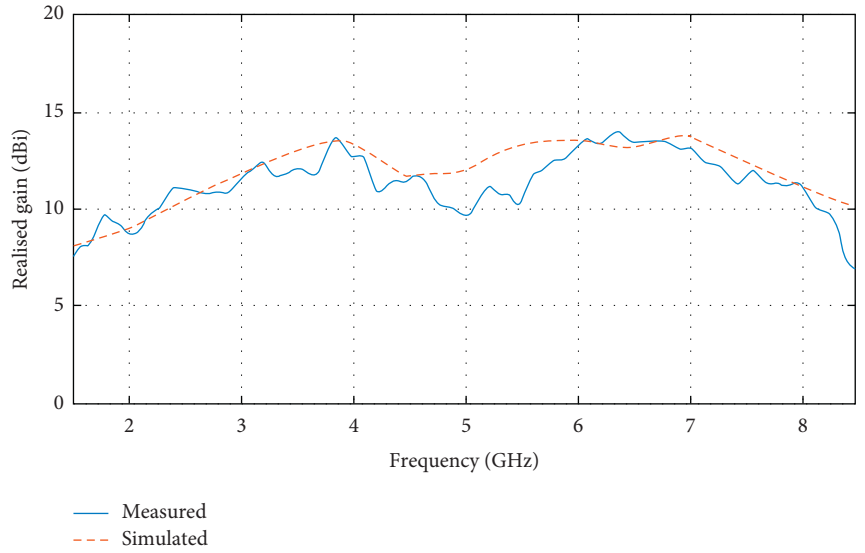

Figure 10: The simulated and measured gain for the antenna array.

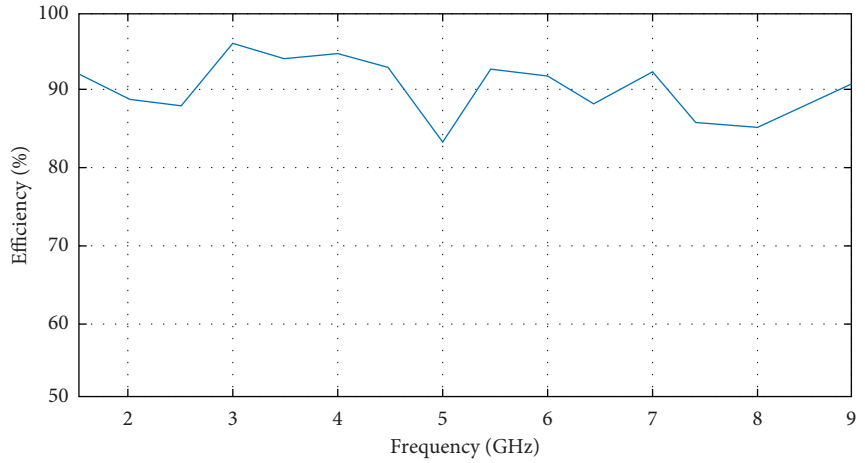

Figure 11: The simulated total efficiency of the antenna array.

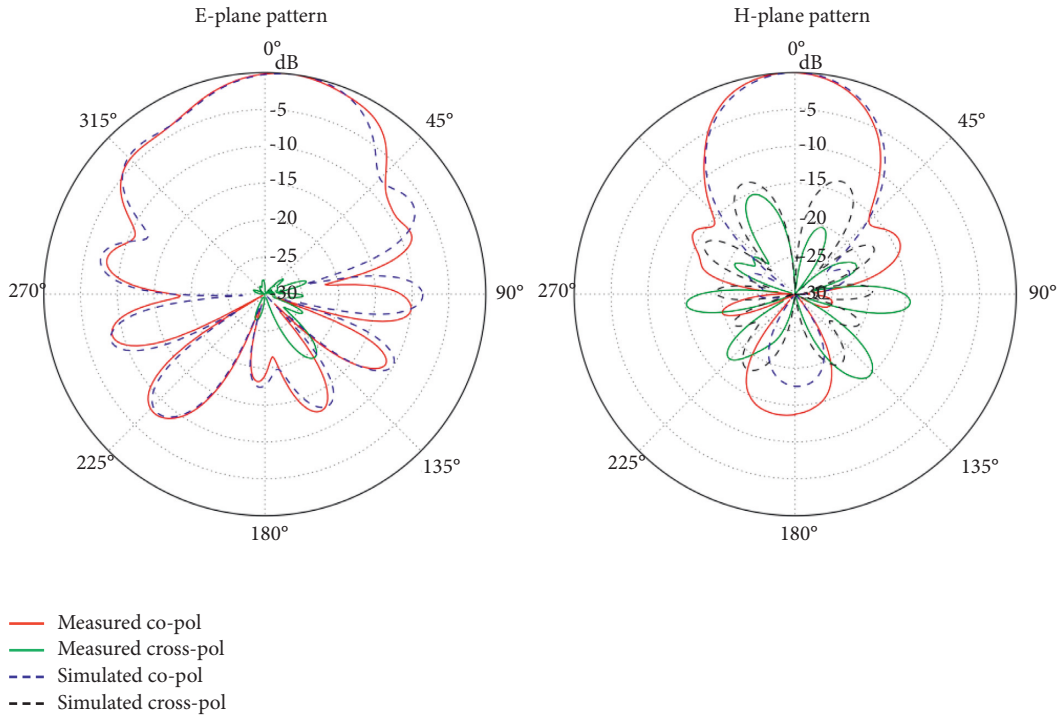

Figure 12: The radiation pattern at 2 GHz.

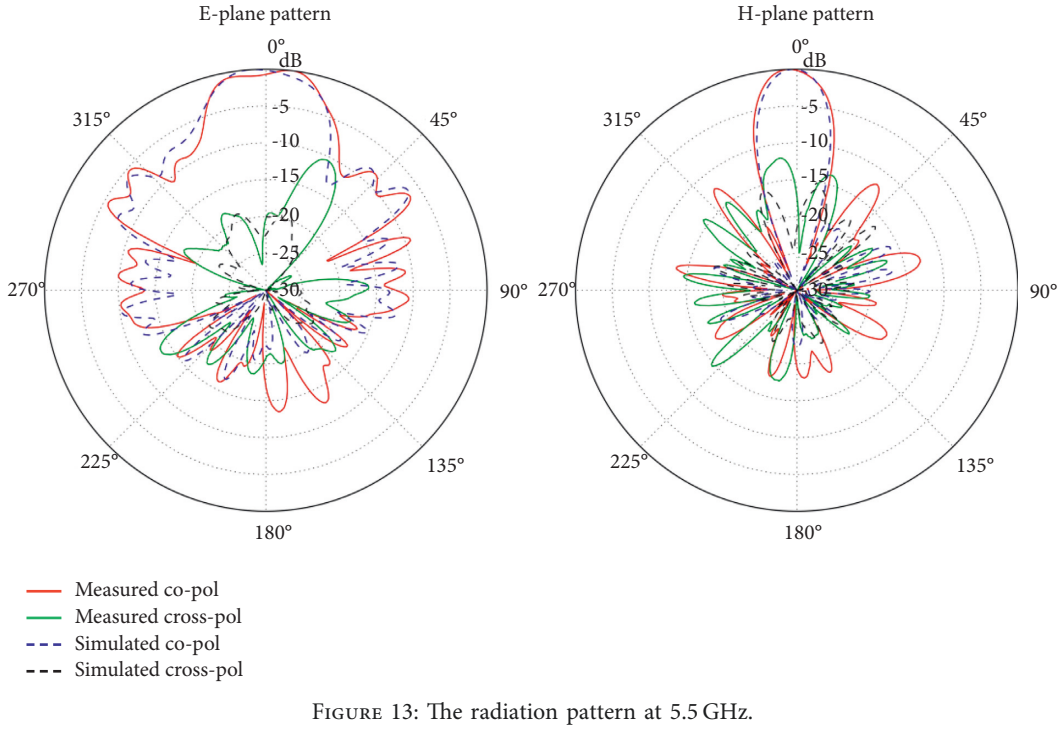

Figure 13: The radiation pattern at 5.5 GHz.

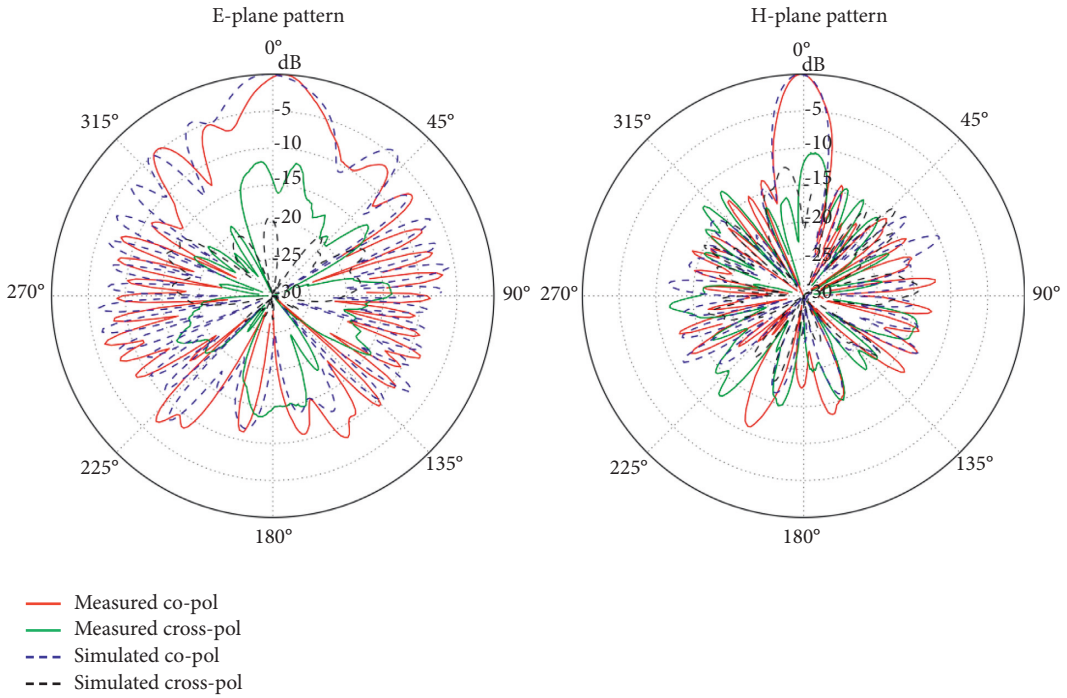

Figure 14: The radiation pattern at 8 GHz.

Table 3: Comparison of different four element wideband arrays.

	Frequency band (GHz)	Useable bandwidth (%)	Maximum gain (dBi)
UWB monopole [4]	2.35–6.1	88.76	10.5
Vivaldi array [5]	3.4–8.3	83.80	12.6
Compact wideband array [6]	8.9–10.9	20.2	10.6
SIW fed array [7]	11.2–13.6	19.35	17.1
Magneto-electric-like array [8]	24.5–40	48	12.65
Proposed antenna array	1.3–8	144.09	13.8

4. Conclusion

Individual Vivaldi antennas are generally capable of achieving bandwidths in excess of 100%. A prototype four element uniform linear array of Vivaldi antennas fed with a wideband corporate feed network was presented. The wideband properties of microstrip-to-slotline transitions were exploited to design a four element corporate feed network consisting of a CPW-to-slotline transition and two slotline-to-microstrip line transitions. The Vivaldi antenna array achieved an impedance bandwidth with VSWR below 2.5 : 1, as well as stable radiation patterns from 1.3 GHz to 8 GHz, resulting in a useable bandwidth of 144%. The proposed antenna array achieved a greater bandwidth and higher gain compared to similar wideband antenna arrays from literature.

Data Availability

Data are available on request from the corresponding author: wimpie@up.ac.za.

Disclosure

Natasha Antoinette Hall (u14007593@tuks.co.za) and Johan Joubert (jjoubert@up.ac.za) are the co-first authors.

Conflicts of Interest

The authors declare that they have no conflicts of interest.

References

[1] E. W. Reid, L. Ortiz-Balbuena, A. Ghadiri, and K. Moez, "A 324-element Vivaldi antenna array for radio astronomy instrumentation," *IEEE Transactions on Instrumentation and Measurement*, vol. 61, no. 1, pp. 241–250, 2012.

[2] H. Legay and L. Shafai, "A self-matching wideband feed network for microstrip arrays," *IEEE Transactions on Antennas and Propagation*, vol. 45, no. 4, pp. 715–722, 1997.

[3] D. Zhai, C. Zhang, Z. Yang, and S. Hu, "Design of the antenna array with a novel feeding network," in *Proceedings of the 2012 International Conference on Microwave and Millimeter Wave Technology (ICMMT)*, pp. 1–4, 2012.

[4] C. X. Zhang, Y. Q. Zhuang, X. K. Zhang, and L. Hu, "An UWB microstrip antenna array with novel corporate-fed structure," *Progress In Electromagnetics Research C*, vol. 52, pp. 7–12, 2014.

[5] B. Xiao, H. Yao, M. Li, J. S. Hong, and K. L. Yeung, "Flexible wideband microstrip-slotline-microstrip power divider and its application to antenna array," *IEEE Access*, vol. 7, pp. 143973–143979, 2019.

[6] F. Karami, P. Rezaei, A. Amn-e-Elahi, and J. S. Meiguni, "A compact and wideband array antenna with efficient hybrid feed network," *International Journal of RF and Microwave Computer-Aided Engineering*, vol. 30, no. 11, pp. 1–8, 2020.

[7] F. Karami, P. Rezaei, A. Amn-e-Elahi, A. Abolfathi, and A. A. Kishk, "Broadband and efficient patch array antenna fed by SIW feed network for Ku-band satellite applications," *International Journal of RF and Microwave Computer-Aided Engineering*, vol. 31, no. 9, pp. 1–14, 2021.

[8] N. Zhang, Z. Yue, Y. Liu, Z. Xue, and Y. Jia, "A wideband low-profile millimeter-wave magneto-electric dipole-like array with low transmission loss feed network," *IEEE Antennas and Wireless Propagation Letters*, vol. 21, no. 2, pp. 277–281, 2022.

[9] T. H. Chio and D. Schaubert, "Parameter study and design of wide-band widescan dual-polarized tapered slot antenna arrays," *IEEE Transactions on Antennas and Propagation*, vol. 48, no. 6, pp. 879–886, 2000.

[10] D. Systèmes, "CST Studio suite electromagnetic field simulation software," 2021, https://www.3ds.com/products-services/%20simulia/products/cst-studio-suite/.